

Published in final edited form as:

Cancer Res. 2018 March 01; 78(5): 1253–1265. doi:10.1158/0008-5472.CAN-17-1547.

Therapy-educated mesenchymal stem cells enrich for tumor initiating cells

Michael Timaner¹, Nitzan Letko-Khait², Ruslana Kotsifruk¹, Madeleine Benguigui¹, Ofrat Beyar-Katz¹, Chen Rachman-Tzemah¹, Ziv Raviv¹, Tomer Bronshtein², Marcelle Machluf², and Yuval Shaked^{1,*}

¹Cell Biology and Cancer Science, Rappaport Faculty of Medicine, Technion – Israel Institute of Technology, Haifa, Israel

²The Laboratory for Cancer Drug Delivery & Cell Based Technologies, Faculty of Biotechnology and Food Engineering, Technion – Israel Institute of Technology, Haifa, Israel

Abstract

Stromal cells residing in the tumor microenvironment contribute to the development of therapy resistance. Here we show that chemotherapy-educated mesenchymal stem cells (MSCs) promote therapy resistance via crosstalk with tumor-initiating cells (TICs), a resistant tumor cell subset that initiates tumorigenesis and metastasis. In response to gemcitabine chemotherapy, MSCs colonized pancreatic adenocarcinomas in large numbers and resided in close proximity to TICs. Furthermore, gemcitabine-educated MSCs promoted the enrichment of TICs in vitro and enhance tumor growth in vivo. These effects were dependent on the secretion of CXCL10 by gemcitabine-educated MSCs and subsequent activation of the CXCL10-CXCR3 axis in TICs. In an orthotopic pancreatic tumor model, targeting TICs using nano-vesicles (called nano-ghosts) derived from MSC membranes and loaded with a CXCR3 antagonist enhanced therapy outcome and delayed tumor re-growth when administered in combination with gemcitabine. Overall, our results establish a mechanism through which MSCs promote chemoresistance, and propose a novel drug delivery system to target TICs and overcome this resistance.

Introduction

Despite ample medical advancements, tumor resistance to commonly used anti-cancer therapies remains a major obstacle in clinical oncology. Various possible mechanisms have been proposed to explain drug resistance. For example, the accumulation of aberrant mutations in growth-related genes activates intrinsic pathways in tumor cells or mutations that affect drug uptake, ultimately resulting in therapy resistance (1). In addition, a growing body of evidence suggests that various cell types residing in the tumor microenvironment also contribute to drug resistance (2–4). It has been shown that upon treatment with chemotherapy or vascular-disrupting agents, several types of bone marrow derived cells

*Corresponding author: Yuval Shaked, Ph.D., Department of Cell Biology and Cancer Science, Rappaport Faculty of Medicine, Technion - Israel Institute of Technology, 1 Efron St. Bat Galim, Haifa, Israel, 31096, Office: 972-4-829-5215, yshaked@tx.technion.ac.il.

Conflict of interest: TB and MM hold a patent on Nano-Ghosts.

(BMDCs), including monocytes and endothelial progenitor cells, home to the treated tumor site and contribute to tumor re-growth by promoting angiogenesis (5–7). Other cells, such as macrophages secrete a variety of factors or enzymes in response to chemotherapy, thereby promoting tumor cell dissemination or protecting tumor cells from the cytotoxic effects of the drug (8–10). Thus, it is clear that the tumor microenvironment plays a significant role in determining tumor fate, especially following conventional therapy.

Mesenchymal stem cells (MSCs) are multipotent stem cells that are able to differentiate into various types of connective tissue cells, including osteoblasts, adipocytes, chondroblasts, fibroblasts and pericytes (11). In tumors, MSCs home to different tumor types including colon, breast, ovarian and lung carcinomas as well as gliomas (12). In desmoplastic tumors, e.g., pancreatic cancer, MSCs secrete GM-CSF and other factors which contribute to tumor cell proliferation, invasion and metastasis (13). Thus, MSCs are an important cell type residing in the tumor microenvironment with pro-tumorigenic abilities. Roodhart *et al.* demonstrated that MSCs promote drug resistance and tumor re-growth in response to chemotherapy, similarly to other stromal cells (14). Specifically, they found that MSCs exposed to cisplatin secrete polyunsaturated fatty acids (12-oxo-5,8,10-heptadecatrienoic acid [KHT], and hexadeca-4,7,10,13-tetraenoic acid [16:4(n-3)]) which protect tumor cells from the cytotoxic effects of the drug through various mediators (14). However, the exact mechanisms by which MSCs contribute to drug resistance and the direct mediators involved in such a process have not been elucidated.

A small sub-population of cancer cells termed cancer stem-like cells or tumor initiating cells (TICs) have been shown to possess stem-like properties. Owing to their ability to self-renew and differentiate, TICs are believed to be responsible to the overall heterogeneity of cancer cells (15). TICs were initially identified in human tumor xenografts implanted in mice. Recent studies have demonstrated that these cells can be isolated or enriched from established human cancer cell lines as well. TIC-enriched cultures grow as tumorspheres and express specific stem cell surface markers, and exhibit elevated aldehyde dehydrogenase activity (16,17). Chan *et al.* recently demonstrated that fibroblasts pre-exposed to chemotherapy such as doxorubicin, paclitaxel or cyclophosphamide promote the enrichment of the TIC population in tumors, leading to tumor re-growth (18). In addition, TICs have been shown to resist cytotoxic agents e.g., chemotherapy, partially due to their slow proliferation rate and high expression of p21 and p53 (19). Thus, current efforts are focused on identifying drugs that specifically target TICs in order to inhibit re-growth and resistance of tumors thereby enhance treatment outcome.

Here we investigated whether TIC enrichment in treated tumors is dependent on MSC. We found that MSCs exposed to gemcitabine chemotherapy secrete increased levels of CXCL10 leading to the enrichment of TICs *in vitro* and *in vivo*, specifically in desmoplastic pancreatic tumors. As drug accumulation in such tumors is poor (20), we employed an MSC-derived nano-ghost (NG) system to deliver a drug that disrupts the CXCL10-CXCR3 axis in treated tumors, and to delay drug resistance. This NG systems is based on nano-vesicles produced from the cytoplasmic membranes of MSCs, and was previously shown to retain MSCs targeting capabilities towards diverse tumor models while allowing safe and effective targeted delivery of bioactive compounds thereto (21,22). Our study demonstrates a

potential therapeutic intervention that can be combined with conventional chemotherapy in order to delay tumor recurrence.

Materials and Methods

Tumor cell cultures

Human U-87MG glioblastoma, HT29 colon carcinoma, A549 non-small cell lung carcinoma, MCF7 breast carcinoma and PANC1, MIA PaCa-2, and BxPC3 pancreatic adenocarcinoma cell lines were purchased in 2015 from the American Type Culture Collection (ATCC, USA). All human cell lines were last authenticated in 2015 by Genetica DNA Laboratories (a LabCorp Specialty Testing Group); using analytical procedures for DNA extraction, polymerase chain reaction and capillary electrophoresis on a 3130xl genetic analyzer (Applied Biosystems), the results of which were confirmed by known repository cell line databases with a match of over 80%. The cells were passaged in culture for no more than 4 months after being thawed from authentic stocks, and were regularly tested and found to be mycoplasma-free (EZ-PCR mycoplasma test kit, Biological industries). Cells were cultured in Dulbecco's modified eagle medium (DMEM) supplemented with 10% fetal bovine serum (FBS), 1% L-glutamine, 1% sodium-pyruvate and 1% penicillin-streptomycin (Biological Industries, Israel). All cells were cultured at 37°C in 5% CO₂.

For in vitro experiments, cells were co-cultured in serum-free medium with untreated or chemotherapy-educated MSC in a 10:1 ratio, or with conditioned medium (CM) derived from untreated or chemotherapy-educated MSCs. In some experiments, serum-free medium was supplemented with CXCL10, IL-3, IL-15 or dipeptidyl-peptidase IV (DPPIV) at concentrations of 10-100ng/ml, anti-hCXCL10 (1µg/ml) or a small molecule blocking CXCR3, AMG487 (1µM; R&D systems). After 3 days, cultures were evaluated for TIC enrichment using the aldehyde dehydrogenase (ALDH) activity, side population (SP) assays and immunophenotype analysis as described below.

The generation of TIC-enriched cultures

TIC-enriched cultures were generated from standard cultures of the various cell lines adapted for growth as non-adherent tumor spheres under specific growth conditions as previously described (17). For more details see Supplemental Materials and Methods.

The generation of chemotherapy-educated MSC or MSC-derived conditioned medium

Human bone marrow MSCs (LONZA, Switzerland) were cultured in minimum essential medium-alpha (MEM α) supplemented with 10% FBS 1% L-glutamine, 1% sodium-pyruvate, and 1% streptomycin. Medium was replaced every 3 days, and cells were maintained in culture for up to 7 passages. MSC phenotype was assessed by flow cytometry as described below.

To generate chemotherapy-educated MSCs, cultured MSCs were exposed to paclitaxel (100nM), gemcitabine (10nM), cisplatin (10µM) or vehicle control for 24 hours. In some experiments, MSCs were exposed to gemcitabine at a dose of 20µM for 30 min, as

previously described (23). To generate MSC-derived CM, the chemotherapy-educated MSCs (as above) were re-seeded in serum-free medium at a concentration of 1×10^5 cells/ml. After 72 hours, CM was collected.

Animal tumor models and treatment protocols

The use of animals and experimental protocols were approved by the Animal Care and Use Committee of the Technion. PANC1 human pancreatic carcinoma cells (5×10^6) and A549 human non-small cell lung carcinoma cells (5×10^6) were subcutaneously injected into the flanks of 8-10 week-old SCID mice (Harlan, Israel). Tumor size was assessed regularly with Vernier calipers using the formula $\text{width}^2 \times \text{length} \times 0.5$. Mice were treated with gemcitabine (500 mg/kg) or vehicle control. In some experiments, mice were injected through the tail vein with untreated or gemcitabine-educated MSCs (1×10^5). To obtain an orthotopic pancreatic tumor model, the peritoneum was exposed and PANC1 cells (5×10^5) either tagged with luciferase or not, were directly injected to the pancreas of 8-10 week old SCID mice. Subsequently, the skin was sutured. Tumor size was monitored weekly using micro-ultrasound Vevo2100 system (Fujifilm VisualSonics, Canada) and IVIS 200 (PerkinElmer, MA). Mice were sacrificed at endpoint and tumors were processed as described below.

Immunohistochemistry

Tumor cryosections ($10 \mu\text{m}$) were stained as previously described (6). To identify human pancreatic TICs, sections were stained with PE-conjugated antibodies against human prominin-1 (CD133, 1:250, Macs MiltenyiBiotec). To identify MSCs, sections were stained with APC-conjugated antibodies against endoglin (CD105, 1:200, BioLegend) and FITC-conjugated antibodies against α -smooth muscle actin (α SMA, 1:200, Sigma-Aldrich, Israel). Tumor sections were analyzed with a LSM 700 Zeiss confocal microscope (Zeiss, Germany). Apoptotic cells were detected by terminal deoxynucleotidyl transferase-mediated dUTP nick end labeling (TUNEL, Roche Diagnostics, Indianapolis, IN) according to the manufacturer's instructions. Controls were immunostained with a secondary antibody alone.

Aldehyde dehydrogenase and side population assays

TIC enrichment was assessed by ALDH activity (24), and SP (25) assays. For more details see Supplemental Materials and Methods.

Cell viability by AlamarBlue assay

Cell viability was assessed using the metabolic indicator dye AlamarBlue (AbD Serotech Ltd.) as described (8). For more details see Supplemental Materials and Methods.

Western blot analysis

PANC1 cells cultured in 60 mm plates were serum-starved overnight. Cells were then either left untreated or incubated for 1 hour with 50ng/ml CXCL10 or CM of control or gemcitabine-educated MSCs. Cells were harvested and lysed in RIPA lysis buffer containing 5M NaCl, 0.5M EDTA, 1M Tris, 1% NP-40, 0.5% sodium deoxycholate, 0.1% SDS. Cell lysates were separated by 10%SDS-PAGE and proteins were electrotransferred to nitrocellulose membranes. Membranes were hybridized with the following primary

antibodies: mouse anti-PI3K (p85) (1:1000, Abcam, UK), mouse anti-AKT (1:1000, Cell Signaling), rabbit anti-phospho-AKT (Ser473) (1:500, Cell Signaling), mouse anti-phospho-ERK (1:1000, Sigma Aldrich), rabbit anti-p44/42 MAPK (ERK 1/2) (1:1000, Cell Signaling), rabbit anti-STAT1 (1:1000, Cell Signaling), rabbit anti-phospho-STAT1 (1:1000, Cell Signaling), rabbit anti-STAT3 (1:1000, Cell Signaling), rabbit anti-phospho-STAT3 (1:1000, Cell Signaling). Actin served as a loading control. Subsequently, membranes were incubated with HRP-conjugated goat anti-mouse and goat-anti-rabbit secondary antibodies (1:5000, Sigma Aldrich). Proteins were detected by enhanced chemiluminescence (Biological Industries).

Flow cytometry analysis

Tumors were prepared as single cell suspensions as previously described (26). Cells were immunostained with fluorescently-labeled monoclonal antibodies against the following markers: CD133-Phycoerythrin (PE), CD44-Allophycocyanin (APC), CD24-PE or CD24-Fluorescein isothiocyanate (FITC), CD105-FITC, CD73-Pacific Blue (PB), Sca1-PE, Gr-1-Brilliant violet (BV) and CD45-APC-Cy7. Monoclonal antibodies were purchased from BD Biosciences, Biolegend, R&D systems and Macs Militenyi Biotec, and used according to the manufacturer's instructions. TICs of U-87MG and A549 cells were defined as CD133+ (17). TICs of HT29 cells were defined as CD133⁺/CD44⁺. TICs of MCF7 cells were identified as CD44⁺/CD24^{-low}, as previously described (16). TIC of pancreatic cells were defined as CD133⁺, CD44⁺/CD133⁺, or CD44⁺/CD24⁺ as previously described (17,18). MSCs were defined as CD105⁺/CD73⁺/CD44⁺/Sca1⁺/CD11b⁻/CD45⁻ cells. For cell apoptosis 7AAD was used. At least 200,000 events were acquired using a Cyan ADP flow cytometer and analyzed with Summit Version 3.4 software (Beckman Coulter).

Cytokine array

CM from gemcitabine-educated or control MSCs were applied to a proteome profiler human XL cytokine array (ARY022B, R&D systems, MN) in accordance with the manufacturer's instruction. The signals corresponding to each factor in the array were quantified by densitometry analysis. The ratio between the expression levels of the various factors secreted by gemcitabine-educated and untreated MSCs was calculated. CXCL10 levels in CM were validated using a specific enzyme-linked immunosorbent assay (ELISA) kit (DY266, R&D systems, MN). The ELISA experiments were carried out in triplicate, and analyzed as mean \pm SD.

Nano-ghost production and administration

NG production from bone marrow-derived MSCs, their labeling with fluorescent lipophilic membrane tracer, DiO, for *in vivo* follow up, and their characterization (size, surface charge, lipid and protein content and composition) were performed as previously described (21,22). For more details see Supplemental Materials and Methods.

Statistical analysis

Data are expressed as mean \pm standard deviation (SD) unless otherwise indicated as standard error (SE). The statistical significance of differences was assessed by one-way ANOVA,

followed by Tukey ad hoc statistical test using GraphPad Prism 5 software (La Jolla, CA). Student t-test was used in some experiments when comparing only two groups. Differences between all groups were compared with each other, and were considered significant at p values below 0.05.

Results

MSCs home to tumors and reside in close proximity to TICs following gemcitabine therapy

Chemotherapy-educated MSCs have been shown to contribute to drug resistance and tumor re-growth (14). However, their effect on TICs has not been studied. To investigate the possible crosstalk between MSCs and TICs, and to determine whether this crosstalk contributes to therapy resistance, we first characterized the spatial relationship between these two cell types in response to chemotherapy. To this end, human pancreatic adenocarcinoma cells (PANC1, 5×10^6) or non-small cell lung carcinoma cells (A549, 5×10^6) were implanted into the flanks of 8-10 week old SCID mice. When tumors reached 500 mm^3 , mice were treated with 500 mg/kg gemcitabine, and three days later tumors were removed. Tumors were sectioned and subsequently immunostained for CD105 and α SMA (to identify MSCs) as well as CD133 (to identify TICs). Interestingly, MSCs were found in close proximity to TICs in PANC1 but not A549 tumors following gemcitabine therapy when compared to untreated control tumors (Figure 1A-B). In addition, flow cytometry analysis revealed that the number of MSCs was significantly higher in treated PANC1 tumors in comparison to untreated control tumors (Figure 1C).

To study the effect of gemcitabine-educated MSCs on tumor growth, mice were subcutaneously co-implanted with PANC1 cells together with human MSCs that had been pre-exposed to either gemcitabine (10nM) or vehicle control for 24 hours. Tumor growth was assessed regularly over time. Co-implantation of MSCs increased the rate of tumor growth in comparison to control tumors. Remarkably, tumor growth rate was the highest in mice co-implanted with gemcitabine-educated MSCs (Figure 1D). At end point, tumors were removed and prepared as single cell suspensions for the quantification of TICs by flow cytometry. Tumors from mice co-implanted with PANC1 cells and gemcitabine-educated MSCs exhibited a significant increase in the percentage of TICs, in comparison to tumors from mice implanted with PANC1 cells alone or together with control MSCs (Figure 1E). Parallel results were obtained when PANC1 cells orthotopically implanted into mice, when injected with MSCs exposed to gemcitabine at a dose of $20 \mu\text{M}$ for 30min, as previously reported (23) (Figure S1 A-C). Collectively, these findings suggest that crosstalk between MSCs and TICs in a gemcitabine-treated tumor microenvironment contribute to the TIC population in a pancreatic cancer model.

Gemcitabine-educated MSCs promote TIC enrichment *in vitro*

Next, we sought to determine whether MSC activity directly contributes to TIC enrichment following exposure to chemotherapy. To this end, various human tumor cell lines were cultured in the presence of CM derived from control or gemcitabine-educated MSC cultures. TIC enrichment was evaluated by phenotypic analysis and ALDH and SP functional assays. Of note, MSC viability was not affected by gemcitabine at the concentration used in the

assay (Figure S2A). CM from gemcitabine-educated MSCs promoted enrichment of TICs in PANC1 and MCF7, but not HT29, A549, and U87 cultures compared to CM from control MSCs as assessed by phenotypic characterization, ALDH activity and SP assays (Figure 2A-C and Figure S2B). Such enrichment effects were also found when PANC1 cells were co-cultured with gemcitabine-educated MSCs (Figure 2D). Notably, we verified that MSCs do not express CD133, ruling out the possibility that we detect both TICs and MSCs in our co-culture system (Figure S2C). We also tested TIC enrichment in the presence of CM from MSCs exposed to other chemotherapy drugs. CM from paclitaxel-exposed MSCs enriched TICs in PANC1 but not A549 cultures, whereas CM from cisplatin-exposed MSCs had no effect in either of the cell lines tested (Figure S2D). Of note, the increased percentage of TICs out of the total cell population is partially due to increased apoptosis of non-TICs population in cultures containing CM of gemcitabine-educated MSCs (Figure 2E). Furthermore, TIC-enriched cultures derived from PANC1 and A549 cell lines were resistant to gemcitabine chemotherapy (Figure S2E), similar to previous published studies (27,28). Using different surface marker combinations (CD133+, CD44+/CD133+, or CD44+/CD24+) and tumorsphere assays, we verified that the enrichment of TICs occurs across various pancreatic cell lines. Specifically, PANC1, MIA Paca-2 and to some extent BxPC3 cells were enriched for TICs in the presence of CM from MSCs exposed to gemcitabine at a dose of either 10nM or 20 μ M compared to control (Figures S3-4). Taken together, these results demonstrate that chemotherapy-educated MSCs promote the enrichment of a TIC population in several specific tumor types, such as pancreatic and breast carcinomas, in part via secreted mediators.

Gemcitabine-educated MSCs promote tumor growth in pancreatic adenocarcinoma models

Thus far, our findings demonstrate tumor homing of MSCs in response to chemotherapy, as well as crosstalk between chemotherapy-educated MSCs and TICs, lead to enrichment of the TIC population. To determine whether these phenomena affect tumor growth, PANC1 (5×10^6) or A549 (5×10^6) cells were subcutaneously implanted into the flanks of 8-10 week old SCID mice. When tumors reached a size of 200mm³, human MSCs (1×10^5) that had been pre-exposed to gemcitabine or vehicle control were injected to the tail vein and tumor growth was monitored. In PANC1 tumor-bearing mice, injecting gemcitabine-educated MSCs significantly increased the rate of tumor growth in comparison to the control and untreated MSC groups (Figure 3A). No significant differences were observed between any of the groups in A549 tumor-bearing mice (Figure 3B). At end point, tumors were removed and prepared as single cell suspensions for the quantification of TICs, injected human MSCs and murine MSCs by flow cytometry. PANC1 tumors from mice injected with gemcitabine-educated MSCs exhibited a significant elevation in the level of TICs in comparison to the control and untreated MSC groups, whereas no significant differences were observed between any of the groups in A549 tumors (Figure 3C-D). Notably, injecting human gemcitabine-educated MSCs caused a reduction in the number of murine MSCs in PANC1 but not A549 tumors, suggesting that at least in the PANC1 tumors, the majority of MSCs contributing to tumor growth are the gemcitabine-educated human MSCs and not murine MSCs. Similarly, in an orthotopic pancreatic tumor model using luciferase-tagged PANC1 cells, tumors in mice injected with gemcitabine-educated MSCs exhibited an increased growth rate as assessed by IVIS and micro-ultrasound (Figure S5A-C). In this model, the

number of TICs was increased in tumors from mice injected with gemcitabine-educated MSCs in comparison to control MSCs, although such differences did not reach statistical significance ($p=0.064$). Importantly, the number of injected gemcitabine-educated MSCs was higher than injected control MSCs, indicating that gemcitabine-educated MSCs home to the tumor more than control MSCs (Figure S5D). Overall, these results suggest that gemcitabine-educated MSCs promote tumor growth in PANC1 but not A549 tumor models.

Gemcitabine-educated MSCs promote TIC enrichment via the CXCL10-CXCR3 signaling pathway

Several cytokines and growth factors have been shown to promote TIC enrichment, including those secreted by MSCs (29–31). We therefore sought to identify the factors secreted by gemcitabine-educated MSCs involved in promoting the enrichment of TICs. To this end, CM from gemcitabine-educated or untreated control MSCs was subjected to a cytokine protein array. Among the most relevant factors that were highly expressed (>5 fold) in the CM of gemcitabine-educated MSCs were DPPIV, CD14, TNFRSF8, IL-2, CXCL10, CXCL11, IL-15, IL-1ra, IL-3, IL-16, BAFF, CCL19, RLN2, G-CSF, IL-31, C5/C5a, IL-13, CCL20, IL-34, BDNF, EGF, IL-1 β , Cripto-1, IL-19, MPO, CXCL9, IL-23 and IL-10 (Table S1). Some of these cytokines such as IL-1 β , IL-2, IL-3, and IL-15, are considered to be pro-inflammatory factors, whereas others such as IL-1RA, IL-10, IL-13 and CXCL10, have anti-inflammatory properties (32). The substantial increase in the levels of the latter factors in the array suggests that MSCs can be pro-tumorigenic (MSC-II) as previously described by Waterman et al. (23). Therefore this may underlie their pro-tumorigenic role by inducing TIC enrichment and contributing to chemoresistance. Moreover, since IL-3, IL-15, CXCL10, and DPPIV are known to be associated with TIC enrichment, proliferation and viability (33–35), we chose to further study these four factors in our system. To determine whether they promote TIC enrichment, PANC1 and A549 cells were cultured in the presence of escalating doses of recombinant IL-3, IL-15, CXCL10 or DPPIV. After 3 days, TICs were quantified by flow cytometry. CXCL10 caused a substantial enrichment (over 4-5 fold) of the TIC population in PANC1 but not A549 tumors, whereas DPPIV demonstrated a substantial enrichment of TICs in both cell lines (Figure 4A-B). Using specific ELISA, we validated that the CXCL10 levels are indeed highly elevated in the CM of gemcitabine-educated MSCs in comparison to untreated MSCs (Figure 4C). In addition to PANC1 cells, we also found that CXCL10 induced TIC enrichment in MIA Paca-2 but not BxPC3 cells, and that the expression level of its receptor, CXCR3 (33) is significantly lower in BxPC3 cells (Figure S6 A-B). Importantly, we found that CXCR3 expression in standard and TIC-enriched cultures, was significantly higher in PANC1 cells in comparison to A549 cells (Figure 4D). Next, we neutralized CXCL10 in the CM of gemcitabine-educated MSCs using anti-CXCL10 antibodies and assessed the effect on TIC enrichment in PANC1 and A549 cultures. In the PANC1 culture, neutralizing CXCL10 reversed the effect induced by the CM of gemcitabine-educated MSCs such that the level of TICs was similar to that in control cultures. In the A549 culture, however, neutralizing CXCL10 caused a reduction in the level of TICs in comparison to all other conditions. These results indicate that CXCL10 is involved in TIC enrichment in both cell lines, however in the PANC1 cells cultured with gemcitabine-educated MSCs the enrichment of TICs is mainly mediated by CXCL10 (Figure 4E-F). To further test the effect of the CXCL10-CXCR3 signaling pathway on TIC

enrichment, TIC-enriched cultures derived from PANC1 and A549 cell lines were incubated with CM from gemcitabine-educated MSCs in the presence or absence of AMG487, a specific CXCR3 antagonist. AMG487 caused a significant reduction in the percentage of TICs in the PANC1 but not A549 cultures (Figure 4G), suggesting that CXCR3-mediated signaling promotes TIC enrichment. Several major signaling cascades such as PI3K-AKT, ERK, STAT1 and STAT3 pathways have been implicated in TIC enrichment (36–38). To identify TIC-promoting signaling pathways that are activated downstream to CXCL10/CXCR3, we evaluated the expression levels of a range of signaling proteins and their phosphorylated forms in lysates derived from PANC1 cells cultured in the presence of CM from untreated and gemcitabine-educated MSCs or serum-free medium supplemented with recombinant CXCL10. The level of pSTAT3 was significantly increased in the presence of CM from gemcitabine-educated MSCs in comparison to CM from untreated MSCs and slightly increased in the presence of recombinant CXCL10 in comparison to its control, as shown in the densitometry analysis (Figure 4H and S7). Overall, our findings demonstrate that CXCL10 secreted by gemcitabine-educated MSCs promotes TIC enrichment mainly via the STAT3 signaling cascade.

Combination therapy using gemcitabine and AMG487-loaded nano-ghosts effectively eliminates TICs in pancreatic adenocarcinoma models

Nano-ghosts (NGs) are cellular membrane-based nano-particles generated from different cell types that can serve as a natural tumor-targeting platform (21,22). In light of the close interaction between MSCs and TICs described in our study, we generated NGs from MSCs in order to develop a drug delivery system that homes to the tumor and specifically targets TICs. Previous studies demonstrated that MSC-NGs distribute in the tumor, liver and kidney within the first 24 hours post injection. In such studies, one week after injection, MSC-NGs were found specifically in tumors, suggesting that passive migratory abilities are sufficient for NG tumor homing specificity (21,22). To test the effect of MSC-NG in our system, we first verified that the MSC-derived NGs do not promote TIC enrichment in vitro (Figure 5A). Second, we evaluated the ability of the NGs to accumulate in gemcitabine-treated tumors. To this end, PANC1 cells were subcutaneously implanted into the flanks of 8-10 week old SCID mice. When tumors reached 500mm³, mice were treated with gemcitabine or vehicle control, and 24 hours later, the mice were intravenously injected with DiO-labeled NGs. One week later, tumors were removed and sectioned. Fluorescence confocal microscopy imaging revealed an accumulation of NGs in tumors of both control and gemcitabine-treated mice. Importantly, the accumulation and retention of NGs in tumors from gemcitabine-treated mice was dramatically increased in comparison to tumors from control mice. Furthermore, NGs were also found in close proximity to TICs in tumors from gemcitabine-treated mice (Figure 5B). These results demonstrate that NGs exhibit tumor-homing and TIC-interacting ability following gemcitabine therapy, similar to MSCs.

Next, we loaded the NGs with AMG487 and evaluated their ability to reduce TIC enrichment in PANC1 cultures treated with CM from gemcitabine-educated MSCs. While unloaded NGs had no effect, NG-AMG-487 significantly reduced the percentage of TICs to a similar extent as AMG-487 in its free form (Figure 5C). These results suggest that NG loaded with AMG-487 may serve as an appropriate drug delivery system to eliminate TICs.

Next, we evaluated the therapeutic activity of NG-AMG487 when used in combination with gemcitabine chemotherapy in an orthotopic pancreatic tumor model. To this end, 8-10 week old SCID mice were orthotopically implanted with PANC1 cells in the pancreas. After two weeks, the mice were treated with gemcitabine alone or in combination with NG-AMG487. Gemcitabine was injected weekly a day before the injection of NGs for a 3 week period. Mice administered with the combination therapy exhibited a significant reduction in tumor growth in comparison to untreated mice or mice treated with gemcitabine or NG-AMG487 monotherapies (Figure 6A-C). Of note, NG-AMG487, on its own, had little effect on tumor growth. The differences in tumor growth patterns when comparing between gemcitabine and its combination with NG-AMG487 were observed only at later time points, i.e., 4 weeks after treatment initiation (Figure 6C-D). These results suggest that TICs, which are known to promote tumor cell repopulation and regrowth (19), are targeted by this drug combination. To test this possibility, in a parallel experiment, tumors were removed 4 days after initiation of the treatment protocol, and evaluated for the presence of apoptotic TICs by fluorescence microscopy and flow cytometry. The percentage of apoptotic TICs (CD133+/7AAD+) was significantly higher in the GEM+NG-AMG487 treated group in comparison to all other groups (Figure 6E-F). Overall, these findings suggest that MSC-derived NGs loaded with AMG487 may serve as an effective therapy for eliminating TICs when administered in combination with gemcitabine chemotherapy.

Discussion

Pancreatic adenocarcinoma is considered one of the most lethal cancers with a 5-year survival rate of less than 7%. This is due to its aggressive characteristics and high metastatic grade on diagnosis (39). Among the factors associated with pancreatic tumor aggressiveness and low responsiveness to treatment is dense fibrosis within the tumor. This desmoplastic nature is associated with a stiff microenvironment that obstructs the tumor penetrating ability of oncology drugs (40). Thus, new drug delivery techniques are being developed to increase therapy efficacy for pancreatic cancer. Focusing on MSCs, we demonstrate that they closely interact with TICs in response to chemotherapy and that they enrich TICs by secreting CXCL10. Furthermore, the disruption of the CXCL10-CXCR3 axis in gemcitabine-treated mice inhibits tumor regrowth by eliminating TICs.

Waterman et al., have recently described two phenotypes of MSCs termed pro-inflammatory MSC-I and anti-inflammatory MSC-II. MSC-II home to tumors and promote tumor cell proliferation, invasion and metastasis (41). In addition, Roodhart et al., have demonstrated that following exposure to chemotherapy, MSCs secrete specific fatty acids which contribute to drug resistance (14). However, the precise mechanism underlying the phenomenon of tumor re-growth following therapy has not been fully elucidated. Our study sheds light on how chemotherapy-educated MSCs promote therapy resistance in tumors. We first demonstrate that there are substantial changes in the secretome of MSCs in response to chemotherapy which appear to compose of a mixed population of both pro-inflammatory and anti-inflammatory types, as indicated in (41). Subsequently, we demonstrate that an intimate crosstalk exists between MSCs recruited to the tumor microenvironment and TICs. This results in enrichment of the TIC population, thereby promoting therapy resistance. We further demonstrate that chemotherapy-educated MSCs secrete CXCL10 that activates the

STAT3 signaling pathway in TICs. Disrupting the CXCL10-CXCR3 axis in TICs reverses the enrichment effect of chemotherapy-educated MSCs on the TIC population. Importantly, we demonstrate that the ability of MSCs to promote TIC enrichment is tumor type dependent. Specifically, we show that MSC-dependent TIC enrichment occurs in pancreatic but not lung cancer cells, even though both tumor types express the CXCL10 receptor, CXCR3. It is plausible that the differential expression of CXCR3 isoforms in different tumor types (42) explains the variable effect on enrichment of TICs in such tumors, as we also demonstrated in our study when using different pancreatic cancer cell lines. Overall, our findings demonstrate a crucial role for cytokines and/or chemokines secreted by chemotherapy-educated MSCs in mediating the crosstalk between MSCs and TICs in specific tumor types. .

The activation of various host cells in response to chemotherapy and their impact on tumor re-growth has recently gained significant attention. Shree et al. demonstrated that macrophages exposed to paclitaxel chemotherapy secrete cathepsins which in turn protect tumor cells from the cytotoxic effect of the drug (9). In addition, secretion of cathepsins by paclitaxel-educated macrophages triggers lymphangiogenesis in treated tumors, explaining increased metastasis that sometimes occurs in response to chemotherapy (10). Like macrophages, cancer associated fibroblasts (CAFs) have been shown to support tumor re-growth and resistance to therapy. Chan et al. demonstrated that in response to high dose chemotherapy, CAFs secrete ELR motif-positive chemokines, which in turn activate their receptor, CXCR2, expressed by tumor cells. This activation cascade leads to TIC enrichment and promotes tumor re-growth (18). Notably, the authors suggest that since CAFs are enriched in desmoplastic tumors, they play a major role in promoting TIC enrichment. Our study demonstrated that MSCs can also contribute to TIC enrichment in response to chemotherapy; however, in such enrichment effect is dependent on the tumor type tested. Specifically, A549 tumors did not exhibit increased TIC levels when cultured with CM from gemcitabine-educated MSCs as opposed to PANC1 tumors. Thus, various factors expressed by stromal cells may contribute to TIC enrichment in different tumor types.

MSCs are clinically approved for the treatment of degenerative arthritis and acute graft versus host disease (GvHD), utilizing their anti-inflammatory capacity and using their immune-evasiveness and relative safety effects (43). In cancer, numerous studies have demonstrated the ability of MSCs to home to multiple types of cancers. Building on this ability, MSCs manipulated ex vivo to secrete various biological drugs upon transplantation have been widely investigated as drug delivery vehicles (cell carriers) to improve the specificity and pharmacokinetics of anti-cancer treatments (44). In preclinical studies, MSCs expressing TRAIL/Apo2L were used for the treatment of lung carcinoma by specifically targeting TICs (45). In addition, MSCs expressing various cytokines including IL-2, IL-12, and interferons (α , β , γ) promoted a cytotoxic immune reaction against tumor cells, reduced metastasis and induced tumor cell apoptosis ultimately inhibiting tumor growth and angiogenesis in melanoma, breast carcinoma, glioma, hepatoma and leukemia (46–48). Unfortunately, MSCs as cell carriers have largely failed to meet their expected oncological clinical potential (49). This disappointing result may be associated with the fact that once transplanted and exposed to the patient's own biological milieu, MSCs undergo changes that alter their targeting capabilities and increase their immunogenicity, only permitting them to

exert a short hit-and-run effect (50). Moreover, owing to the natural role of MSCs in protecting tumors from the immune system and facilitating the metastatic process, along with their contribution to TIC enrichment and tumor chemotherapy resistance, MSCs may, counterproductively, promote tumorigenesis (14,29).

To overcome these challenges in drug delivery, we have employed NGs derived from MSCs to target desmoplastic tumors. This system makes use of the unique tumor-targeting capabilities of MSCs. NGs produced from the cytoplasmic membranes of MSCs have been previously reported to safely target various *in vivo* tumor models, including prostate and lung cancers, improving therapeutic outcomes (21,22). Here, we demonstrate that MSC-derived NGs, on their own, do not support TIC enrichment, but home to gemcitabine-treated tumors in large numbers. Furthermore, MSC-NGs loaded with a CXCR3 antagonist disrupt the crosstalk between MSCs and TICs that occurs in response to chemotherapy. Therefore combining these NGs with gemcitabine therapy significantly enhances treatment efficacy and delays tumor re-growth in comparison to gemcitabine monotherapy in mice bearing pancreatic tumors. We found that TICs underwent apoptosis at the treated-tumor site, in the combination therapy. Importantly, these findings further support our hypothesis, corroborated by our previous NG studies (21,22), that MSC tumor-targeting capacity is largely governed by direct cell-cell interactions through membrane proteins, and not by MSC chemotaxis alone.

In summary, our study reveals the interaction between MSCs and TICs in the pancreatic tumor microenvironment. Inhibiting the intimate crosstalk between these two cell types by disrupting the CXCL10-CXCR3 axis ‘sensitizes’ tumor cells to chemotherapy mainly by targeting TICs residing in the treated tumor. Based on the ability of MSCs to specifically home to tumors and target the TIC population, we propose the use of MSC-derived NGs as ‘Trojan horses’. Such NG-based therapy represents a promising strategy to overcome resistance, especially in desmoplastic cancers such as pancreatic adenocarcinomas.

Supplementary Material

Refer to Web version on PubMed Central for supplementary material.

Acknowledgment

This study was supported by research grants from the European Research Council (under the FP-7 program, 260633) and from the Rappaport institute (to Y Shaked); and Ed Satell Fund for Novel Technologies for Cancer and Stem Cell-Based Therapy (to M Machluf).

References

1. Holohan C, Van Schaeybroeck S, Longley DB, Johnston PG. Cancer drug resistance: an evolving paradigm. *Nature reviews Cancer*. 2013; 13(10):714–26. [PubMed: 24060863]
2. Hanahan D, Coussens LM. Accessories to the crime: functions of cells recruited to the tumor microenvironment. *Cancer Cell*. 2012; 21(3):309–22. [PubMed: 22439926]
3. Shaked Y. Balancing efficacy of and host immune responses to cancer therapy: the yin and yang effects. *Nat Rev Clin Oncol*. 2016; 13(10):611–26. [PubMed: 27118493]
4. Katz OB, Shaked Y. Host effects contributing to cancer therapy resistance. *Drug Resist Updat*. 2015; 19:33–42. [PubMed: 25575621]

5. Welford AF, Biziato D, Coffelt SB, Nucera S, Fisher M, Pucci F, et al. TIE2-expressing macrophages limit the therapeutic efficacy of the vascular-disrupting agent combretastatin A4 phosphate in mice. *J Clin Invest.* 2011; 121(5):1969–73. [PubMed: 21490397]
6. Shaked Y, Ciarrocchi A, Franco M, Lee CR, Man S, Cheung AM, et al. Therapy-induced acute recruitment of circulating endothelial progenitor cells to tumors. *Science.* 2006; 313(5794):1785–7. [PubMed: 16990548]
7. Shaked Y, Henke E, Roodhart JM, Mancuso P, Langenberg MH, Colleoni M, et al. Rapid chemotherapy-induced acute endothelial progenitor cell mobilization: implications for antiangiogenic drugs as chemosensitizing agents. *Cancer Cell.* 2008; 14(3):263–73. [PubMed: 18772115]
8. Gingis-Velitski S, Loven D, Benayoun L, Munster M, Bril R, Voloshin T, et al. Host response to short-term, single-agent chemotherapy induces matrix metalloproteinase-9 expression and accelerates metastasis in mice. *Cancer Res.* 2011; 71(22):6986–96. [PubMed: 21978934]
9. Shree T, Olson OC, Elie BT, Kester JC, Garfall AL, Simpson K, et al. Macrophages and cathepsin proteases blunt chemotherapeutic response in breast cancer. *Genes & development.* 2011; 25(23):2465–79. [PubMed: 22156207]
10. Alishekevitz D, Gingis-Velitski Svetlana, Kaidr-Person Orit, Gutter-Kapon Lilach, Scherer Sandra D, Raviv Ziv, Merquiol Emmanuelle, Ben-Nun Yael, Miller Valeria, Rachman-Tzemah Chen, Timaner Michael, et al. Macrophage-induced lymphangiogenesis and metastasis following paclitaxel chemotherapy is regulated by VEGFR3. *Cell reports.* 2016; 17:1344–56. [PubMed: 27783948]
11. Uccelli A, Moretta L, Pistoia V. Mesenchymal stem cells in health and disease. *Nat Rev Immunol.* 2008; 8(9):726–36. [PubMed: 19172693]
12. Reagan MR, Kaplan DL. Concise review: Mesenchymal stem cell tumor-homing: detection methods in disease model systems. *Stem cells.* 2011; 29(6):920–7. [PubMed: 21557390]
13. Waghray M, Yalamanchili M, Dziubinski M, Zeinali M, Erkkinen M, Yang H, et al. GM-CSF Mediates Mesenchymal-Epithelial Cross-talk in Pancreatic Cancer. *Cancer Discov.* 2016; 6(8):886–99. [PubMed: 27184426]
14. Roodhart JM, Daenen LG, Stigter EC, Prins HJ, Gerrits J, Houthuijzen JM, et al. Mesenchymal stem cells induce resistance to chemotherapy through the release of platinum-induced fatty acids. *Cancer Cell.* 2011; 20(3):370–83. [PubMed: 21907927]
15. Visvader JE, Lindeman GJ. Cancer stem cells in solid tumours: accumulating evidence and unresolved questions. *Nature reviews Cancer.* 2008; 8(10):755–68. [PubMed: 18784658]
16. Benayoun L, Gingis-Velitski S, Voloshin T, Segal E, Segev R, Munster M, et al. Tumor-initiating cells of various tumor types exhibit differential angiogenic properties and react differently to antiangiogenic drugs. *Stem cells.* 2012; 30(9):1831–41. [PubMed: 22782858]
17. Benayoun L, Shaked Y. In vitro enrichment of tumor-initiating cells from human established cell lines. *Curr Protoc Stem Cell Biol.* 2013 Chapter 3:Unit 3 7.
18. Chan TS, Hsu CC, Pai VC, Liao WY, Huang SS, Tan KT, et al. Metronomic chemotherapy prevents therapy-induced stromal activation and induction of tumor-initiating cells. *J Exp Med.* 2016; 213(13):2967–88. [PubMed: 27881732]
19. Dean M, Fojo T, Bates S. Tumour stem cells and drug resistance. *Nature reviews Cancer.* 2005; 5(4):275–84. [PubMed: 15803154]
20. Whatcott, CJ., Posner, RG., Von Hoff, DD., Han, H. Desmoplasia and chemoresistance in pancreatic cancer. 2012.
21. Kaneti L, Bronshtein T, Malkah Dayan N, Kovregina I, Letko Khait N, Lupu-Haber Y, et al. Nanoghosts as a Novel Natural Nonviral Gene Delivery Platform Safely Targeting Multiple Cancers. *Nano Lett.* 2016; 16(3):1574–82. [PubMed: 26901695]
22. Toledano Furman NE, Lupu-Haber Y, Bronshtein T, Kaneti L, Letko N, Weinstein E, et al. Reconstructed stem cell nanoghosts: a natural tumor targeting platform. *Nano Lett.* 2013; 13(7):3248–55. [PubMed: 23786263]
23. Grunewald R, Kantarjian H, Du M, Faucher K, Tarassoff P, Plunkett W. Gemcitabine in leukemia: a phase I clinical, plasma, and cellular pharmacology study. *J Clin Oncol.* 1992; 10(3):406–13. [PubMed: 1740680]

24. Ginestier C, Hur MH, Charafe-Jauffret E, Monville F, Dutcher J, Brown M, et al. ALDH1 is a marker of normal and malignant human mammary stem cells and a predictor of poor clinical outcome. *Cell Stem Cell*. 2007; 1(5):555–67. [PubMed: 18371393]
25. Golebiewska A, Brons NH, Bjerkvig R, Niclou SP. Critical appraisal of the side population assay in stem cell and cancer stem cell research. *Cell Stem Cell*. 2011; 8(2):136–47. [PubMed: 21295271]
26. Timaner M, Beyar-Katz O, Shaked Y. Analysis of the Stromal Cellular Components of the Solid Tumor Microenvironment Using Flow Cytometry. *Curr Protoc Cell Biol*. 2016; 70:19 18 1–19 18 12.
27. Quint K, Tonigold M, Di Fazio P, Montalbano R, Lingelbach S, Ruckert F, et al. Pancreatic cancer cells surviving gemcitabine treatment express markers of stem cell differentiation and epithelial-mesenchymal transition. *Int J Oncol*. 2012; 41(6):2093–102. [PubMed: 23026911]
28. Hermann PC, Huber SL, Herrler T, Aicher A, Ellwart JW, Guba M, et al. Distinct populations of cancer stem cells determine tumor growth and metastatic activity in human pancreatic cancer. *Cell Stem Cell*. 2007; 1(3):313–23. [PubMed: 18371365]
29. Liu S, Ginestier C, Ou SJ, Clouthier SG, Patel SH, Monville F, et al. Breast cancer stem cells are regulated by mesenchymal stem cells through cytokine networks. *Cancer Res*. 2011; 71(2):614–24. [PubMed: 21224357]
30. Rasanen K, Herlyn M. Paracrine signaling between carcinoma cells and mesenchymal stem cells generates cancer stem cell niche via epithelial-mesenchymal transition. *Cancer Discov*. 2012; 2(9):775–7. [PubMed: 22969117]
31. Karnoub AE, Dash AB, Vo AP, Sullivan A, Brooks MW, Bell GW, et al. Mesenchymal stem cells within tumour stroma promote breast cancer metastasis. *Nature*. 2007; 449(7162):557–63. [PubMed: 17914389]
32. Turner MD, Nedjai B, Hurst T, Pennington DJ. Cytokines and chemokines: At the crossroads of cell signalling and inflammatory disease. *Biochim Biophys Acta*. 2014; 1843(11):2563–82. [PubMed: 24892271]
33. Li Y, Reader JC, Ma X, Kundu N, Kochel T, Fulton AM. Divergent roles of CXCR3 isoforms in promoting cancer stem-like cell survival and metastasis. *Breast Cancer Res Treat*. 2015; 149(2):403–15. [PubMed: 25537642]
34. Jin L, Lee EM, Ramshaw HS, Busfield SJ, Peoppl AG, Wilkinson L, et al. Monoclonal antibody-mediated targeting of CD123, IL-3 receptor alpha chain, eliminates human acute myeloid leukemic stem cells. *Cell Stem Cell*. 2009; 5(1):31–42. [PubMed: 19570512]
35. Ou X, O'Leary HA, Broxmeyer HE. Implications of DPP4 modification of proteins that regulate stem/progenitor and more mature cell types. *Blood*. 2013; 122(2):161–9. [PubMed: 23637126]
36. Luo ML, Gong C, Chen CH, Hu H, Huang P, Zheng M, et al. The Rab2A GTPase promotes breast cancer stem cells and tumorigenesis via Erk signaling activation. *Cell reports*. 2015; 11(1):111–24. [PubMed: 25818297]
37. Hambardzumyan D, Becher OJ, Rosenblum MK, Pandolfi PP, Manova-Todorova K, Holland EC. PI3K pathway regulates survival of cancer stem cells residing in the perivascular niche following radiation in medulloblastoma in vivo. *Genes & development*. 2008; 22(4):436–48. [PubMed: 18281460]
38. Avalle L, Pensa S, Regis G, Novelli F, Poli V. STAT1 and STAT3 in tumorigenesis: A matter of balance. *Jak-Stat*. 2012; 1(2):65–72. [PubMed: 24058752]
39. Chand S, O'Hayer K, Blanco FF, Winter JM, Brody JR. The Landscape of Pancreatic Cancer Therapeutic Resistance Mechanisms. *Int J Biol Sci*. 2016; 12(3):273–82. [PubMed: 26929734]
40. Neesse A, Michl P, Frese KK, Feig C, Cook N, Jacobetz MA, et al. Stromal biology and therapy in pancreatic cancer. *Gut*. 2011; 60(6):861–8. [PubMed: 20966025]
41. Waterman RS, Tomchuck SL, Henkle SL, Betancourt AM. A new mesenchymal stem cell (MSC) paradigm: polarization into a pro-inflammatory MSC1 or an Immunosuppressive MSC2 phenotype. *PLoS one*. 2010; 5(4):e10088. [PubMed: 20436665]
42. Ma B, Khazali A, Wells A. CXCR3 in carcinoma progression. *Histol Histopathol*. 2015; 30(7):781–92. [PubMed: 25663474]

43. Gao F, Chiu SM, Motan DA, Zhang Z, Chen L, Ji HL, et al. Mesenchymal stem cells and immunomodulation: current status and future prospects. *Cell Death Dis.* 2016; 7:e2062. [PubMed: 26794657]
44. Ashkenazi A, Pai RC, Fong S, Leung S, Lawrence DA, Marsters SA, et al. Safety and antitumor activity of recombinant soluble Apo2 ligand. *J Clin Invest.* 1999; 104(2):155–62. [PubMed: 10411544]
45. Loebinger MR, Sage EK, Davies D, Janes SM. TRAIL-expressing mesenchymal stem cells kill the putative cancer stem cell population. *Br J Cancer.* 2010; 103(11):1692–7. [PubMed: 21063402]
46. Nakamizo A, Marini F, Amano T, Khan A, Studeny M, Gumin J, et al. Human bone marrow-derived mesenchymal stem cells in the treatment of gliomas. *Cancer Res.* 2005; 65(8):3307–18. [PubMed: 15833864]
47. Studeny M, Marini FC, Dembinski JL, Zompetta C, Cabreira-Hansen M, Bekele BN, et al. Mesenchymal stem cells: potential precursors for tumor stroma and targeted-delivery vehicles for anticancer agents. *J Natl Cancer Inst.* 2004; 96(21):1593–603. [PubMed: 15523088]
48. Ren C, Kumar S, Chanda D, Kallman L, Chen J, Mountz JD, et al. Cancer gene therapy using mesenchymal stem cells expressing interferon-beta in a mouse prostate cancer lung metastasis model. *Gene Ther.* 2008; 15(21):1446–53. [PubMed: 18596829]
49. Shah K. Mesenchymal stem cells engineered for cancer therapy. *Advanced drug delivery reviews.* 2012; 64(8):739–48. [PubMed: 21740940]
50. Levy O, Zhao W, Mortensen LJ, Leblanc S, Tsang K, Fu M, et al. mRNA-engineered mesenchymal stem cells for targeted delivery of interleukin-10 to sites of inflammation. *Blood.* 2013; 122(14):e23–32. [PubMed: 23980067]

Significance

Results establish a mechanism by which mesenchyme stem cells in the tumor microenvironment promote chemoresistance, and they propose a novel drug delivery system to overcome this challenge.

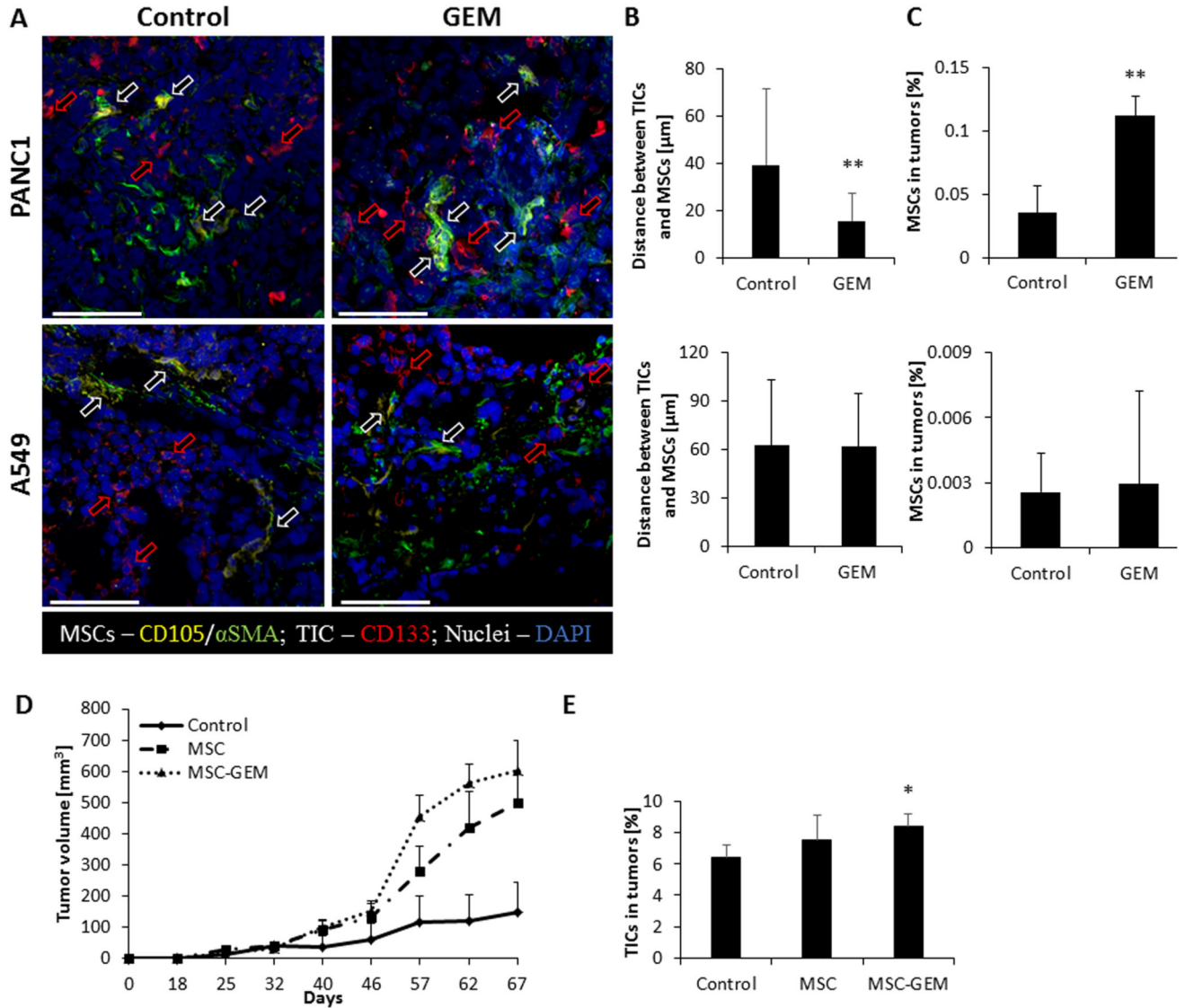


Figure 1. Chemotherapy induces the homing of MSCs to TICs in pancreatic tumors:

(A-C) Eight-to-ten week old SCID mice were subcutaneously implanted with PANC1 or A549 cells (n=5 mice/group). When tumors reached 500mm³, treatment with gemcitabine (500mg/kg) or vehicle control was initiated. After 72 hours the tumors were harvested; half of the tumor was sectioned and the other half was prepared as a single cell suspension. (A) Tumor sections were immunostained using antibodies against CD105 (yellow) and αSMA (green) to identify MSCs, and CD133 (red) to identify TICs. Nuclei were stained with DAPI (blue). Red arrows represent TICs whereas white arrows represent MSCs. Scale bar, 100 μm. (B) The distance between MSCs and TICs was measured and plotted (n>15 fields/group). (C) The percentage of MSCs in tumor single cell suspensions was quantified by flow cytometry. (D-E) Eight-to-ten week old SCID mice were co-implanted with PANC1 (5x10⁶ cells) and human MSCs (5x10⁵ cells). (D) Tumor growth was assessed regularly. Error bars represent SE. (E) At end point, tumors were removed and prepared as single cell

suspensions. The percentage of TICs was assessed by flow cytometry. * $p < 0.05$, ** $p < 0.01$, as assessed by student t-test or one way ANOVA followed by Tukey post-hoc test (when comparing between more than two groups).

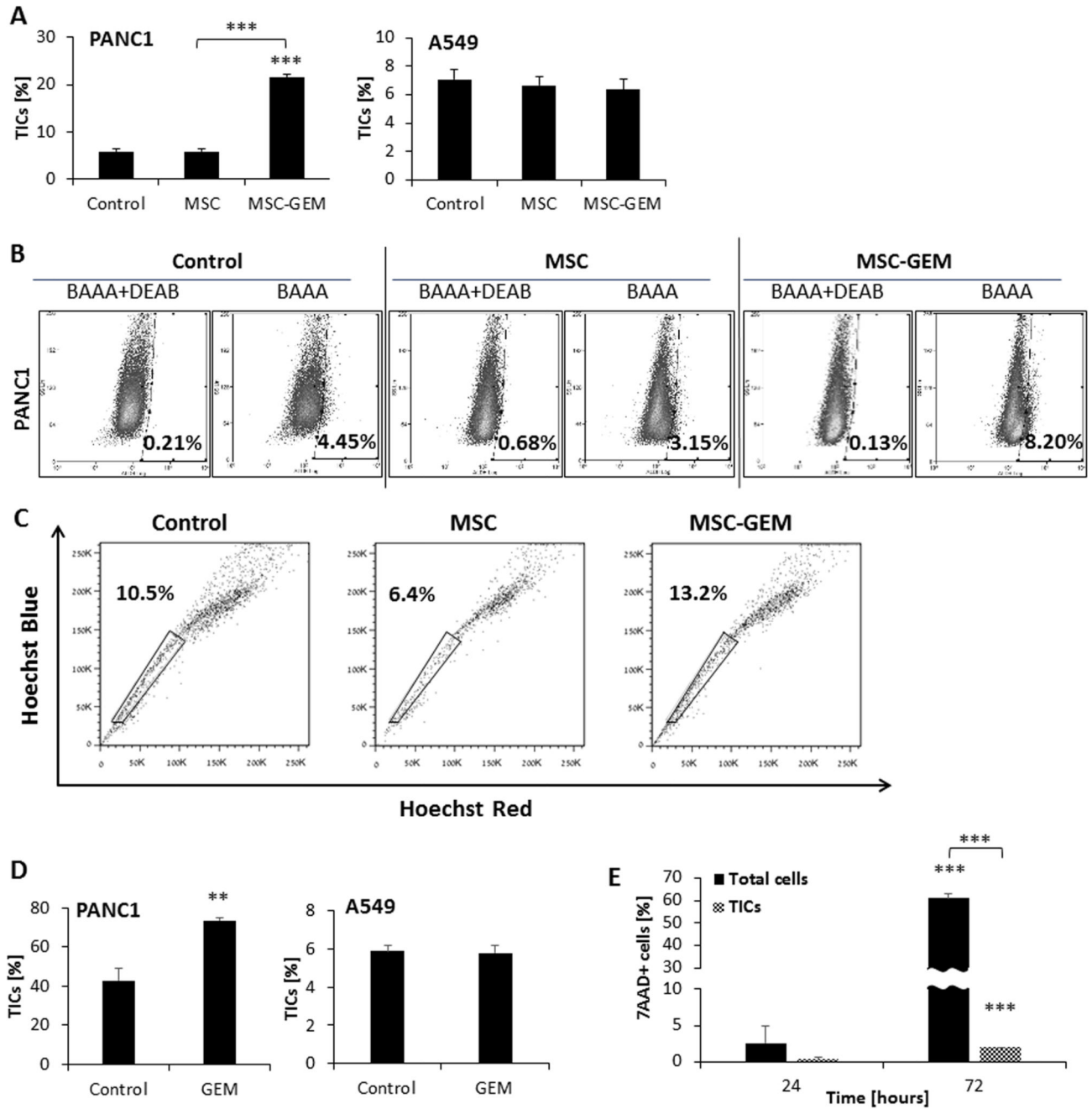


Figure 2. Gemcitabine-educated MSCs promote TIC enrichment in PANC1 but not A549 cultures:

(A) PANC1 and A549 cells were cultured in serum-free medium supplemented with conditioned medium (CM) derived from control or gemcitabine-educated MSC cultures. After 72 hours, the percentage of TICs was assessed by flow cytometry. (B) Aldehyde dehydrogenase (ALDH) activity was evaluated in PANC1 cells treated as in (A). DEAB was used as a negative control. (C) SP assay was assessed on PANC1 cells treated as in (A). (D) PANC1 and A549 cells were co-cultured with MSCs in 1:10 ratio in serum-free conditions for 72 hours. The cultures were then treated with gemcitabine (10 nM) or vehicle control for

72 hours and the percentage of TICs (CD133+) was evaluated by flow cytometry. (E) Standard and TIC-enriched PANC1 cultures were incubated with naïve or gemcitabine-educated MSCs. After 24 or 72 hours, the percentage of apoptotic cells in each culture was assessed by flow cytometry. * $p < 0.05$, ** $p < 0.01$, *** $p < 0.001$, as assessed by student t-test or one way ANOVA followed by Tukey post-hoc test (when comparing between more than two groups).

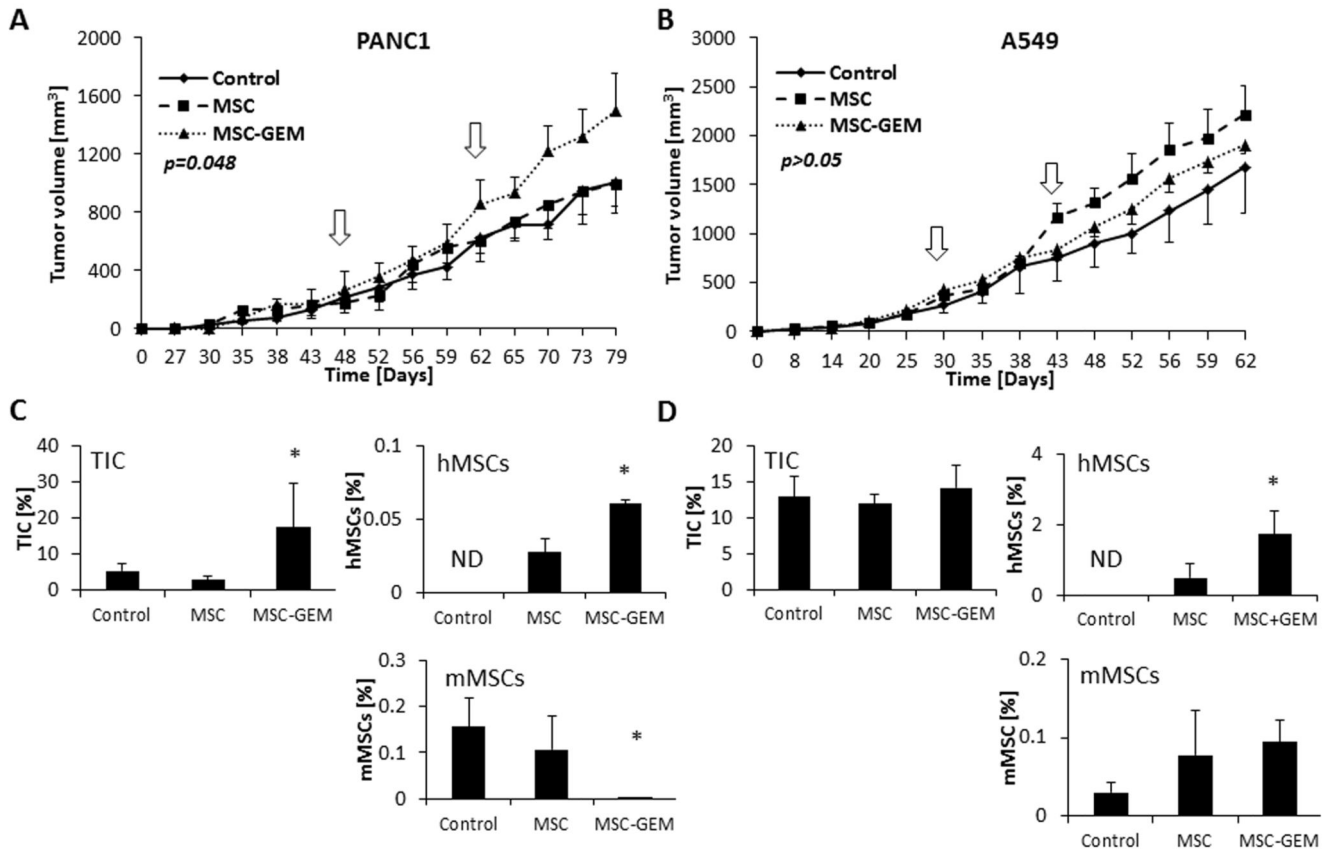


Figure 3. Gemcitabine-educated MSCs promote tumor growth in a pancreatic cancer mouse model.

(A-B) Eight-to-ten week old SCID mice were subcutaneously implanted with PANC1 (A) or A549 (B) cells. When tumors reached 200mm³, mice were either left untreated (control) or were administrated twice (white arrows) with naïve MSCs or gemcitabine-educated MSCs (MSC-GEM). Tumor growth was assessed. Error bars represent SE. (C-D) At end point, mice were sacrificed, tumors were harvested and prepared as single cell suspensions. The percentages of TICs, murine MSCs (mMSC) and human MSCs (hMSC) in PANC1 (C) and A549 (D) tumors were quantified using flow cytometry. ND, not detected. * $p < 0.05$, *** $p < 0.001$, as assessed by one way ANOVA followed by Tukey post-hoc test (when comparing between more than two groups).

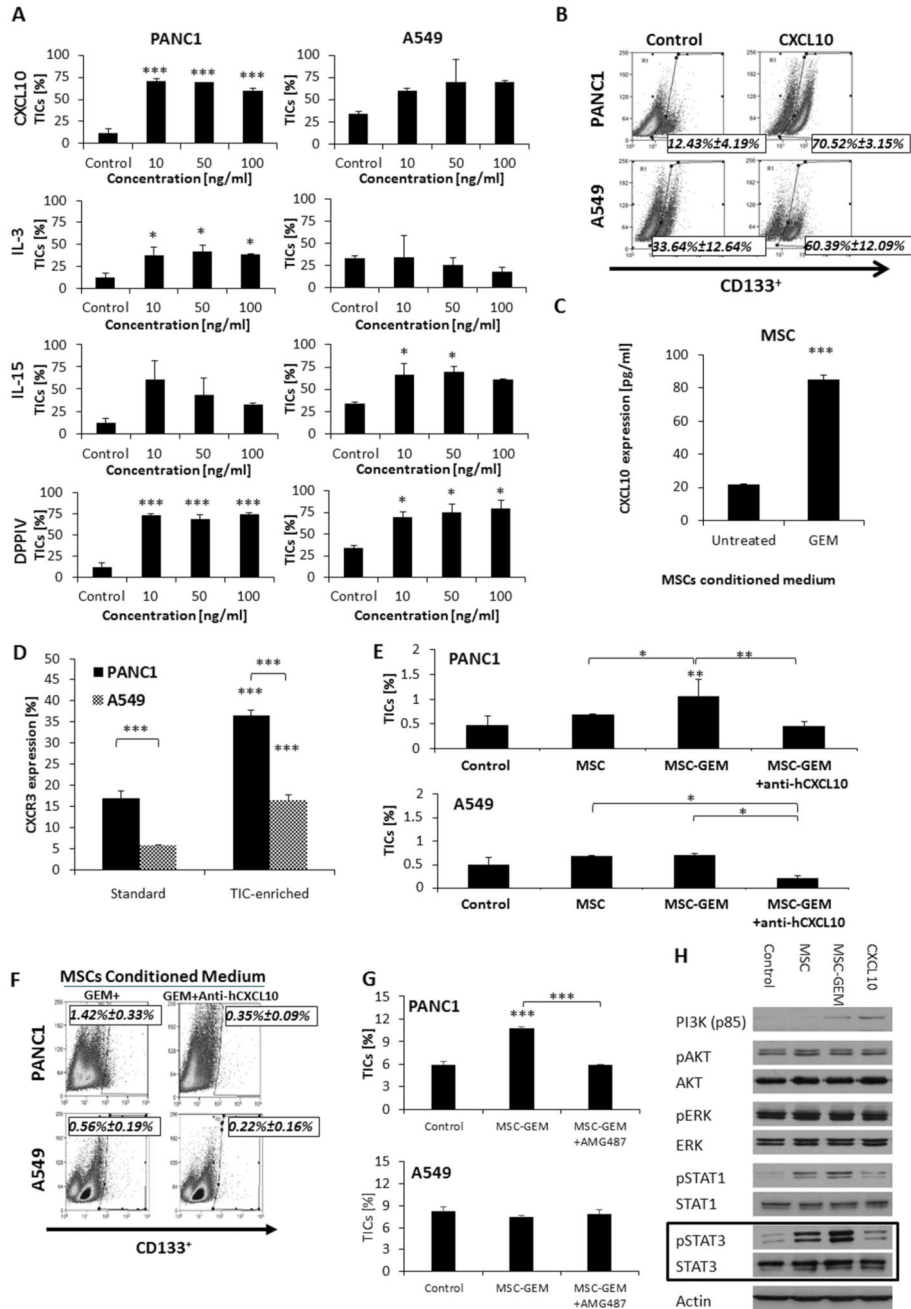


Figure 4. CXCL10 promotes TIC enrichment in PANC1 cultures:

(A) PANC1 and A549 cells were cultured in serum-free medium supplemented with escalating doses of CXCL10, IL-3, IL-15 or DPPIV as indicated. After 3 days, the percentage of TICs in each culture was evaluated by flow cytometry. (B) Representative flow cytometry plots are shown for PANC1 and A549 cultures supplemented with 10 ng/ml CXCL10. (C) MSCs were incubated with vehicle control or gemcitabine (10 nM) for 24 hours, followed by serum-free medium for 72 hours. The level of CXCL10 in conditioned medium was assessed by ELISA. (D) The percentage of cells expressing CXCR3 in standard

and TIC-enriched cultures of PANC1 and A549 cells was evaluated by flow cytometry. (E) PANC1 and A549 cells were cultured in serum-free medium (control) or serum-free medium supplemented with conditioned medium derived from cultures of control MSCs (MSC), gemcitabine-educated MSCs (MSC-GEM) or gemcitabine- and anti-CXCL10-treated MSCs (MSC-GEM+anti-hCXCL10). After 3 days, the percentage of TICs in culture was assessed by flow cytometry. (F) Representative flow cytometry plots are shown for PANC1 and A549 cultures supplemented with conditioned medium of MSCs treated with gemcitabine in the absence or presence of anti-hCXCL10. (G) PANC1 and A549 cells were cultured in serum-free medium (control) or serum-free medium supplemented with conditioned medium derived from gemcitabine-educated MSCs (MSC-GEM) in the absence or presence of the CXCR3 antagonist, AMG487 (1 μ M). After 3 days, the percentage of TICs in each culture was assessed by flow cytometry. (H) PANC1 cells were cultured in serum-free medium supplemented as follows: unsupplemented (control); conditioned medium derived from untreated (MSC) or gemcitabine-educated MSCs (MSC-GEM); CXCL10 (50 ng/ml). After 1 hour, cells were harvested and the expression levels of the indicated factors were assessed by Western blot. * p <0.05, ** p <0.01, *** p <0.001, as assessed by one way ANOVA followed by Tukey post-hoc test (when comparing between more than two groups).

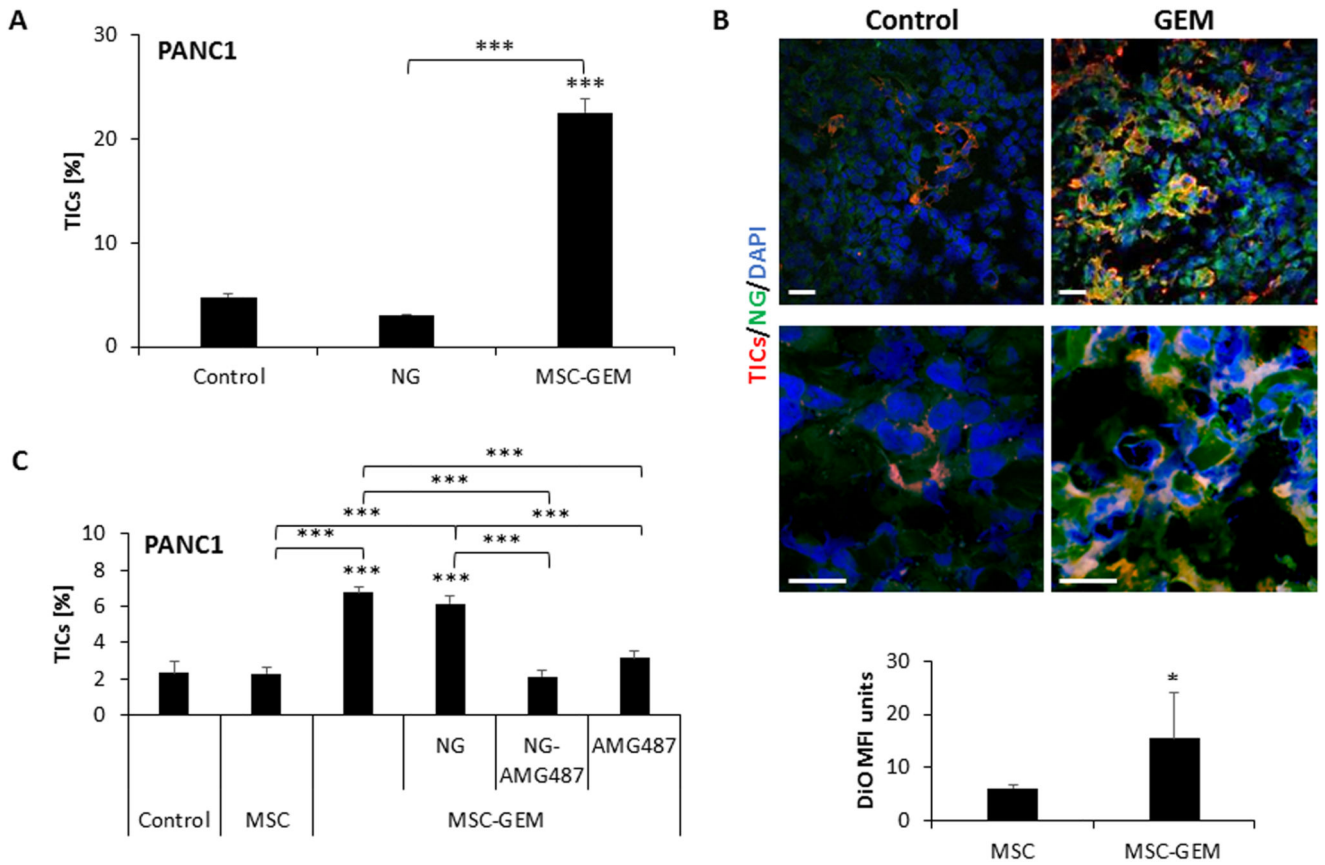


Figure 5. MSC-derived nano-ghosts home to PANC1 tumors in response to gemcitabine therapy: (A) PANC1 cells were cultured in serum-free medium supplemented as follows: unsupplemented (control); MSC-derived nano-ghosts (NG); and CM derived from gemcitabine-educated MSCs (MSC-GEM). After 3 days, the percentage of TICs in each culture was evaluated by flow cytometry. (B) Eight-to-ten week old SCID mice were orthotopically implanted with PANC1 cells (5×10^5 cells/mouse) into the pancreas. After 4 weeks, the mice were treated with gemcitabine (500mg/kg) or vehicle control. Twenty-four hours later, mice were intravenously injected with DiO-labelled NGs. After 1 week, mice were sacrificed and tumors were sectioned. Tumor sections were immunostained with antibodies against CD133 to detect TICs (red). Nuclei were stained with DAPI (blue). The mean fluorescence intensity (MFI) of the DiO signal (green) was calculated. Scale bar, 100 μ m. (C) PANC1 cells were cultured in serum-free medium supplemented as follows: unsupplemented (control), conditioned medium from untreated MSCs (MSC), CM from gemcitabine-educated MSCs (CM-MSC-GEM) alone or in combination with MSC-derived nano-ghosts (NG), AMG487-loaded NGs (NG-AMG487), or free AMG487 (1 μ M). After 3 days, the percentage of TICs in each culture was evaluated by flow cytometry. * $p < 0.05$, ** $p < 0.01$, *** $p < 0.001$, as assessed by student t-test or one way ANOVA followed by Tukey post-hoc test (when comparing between more than two groups).

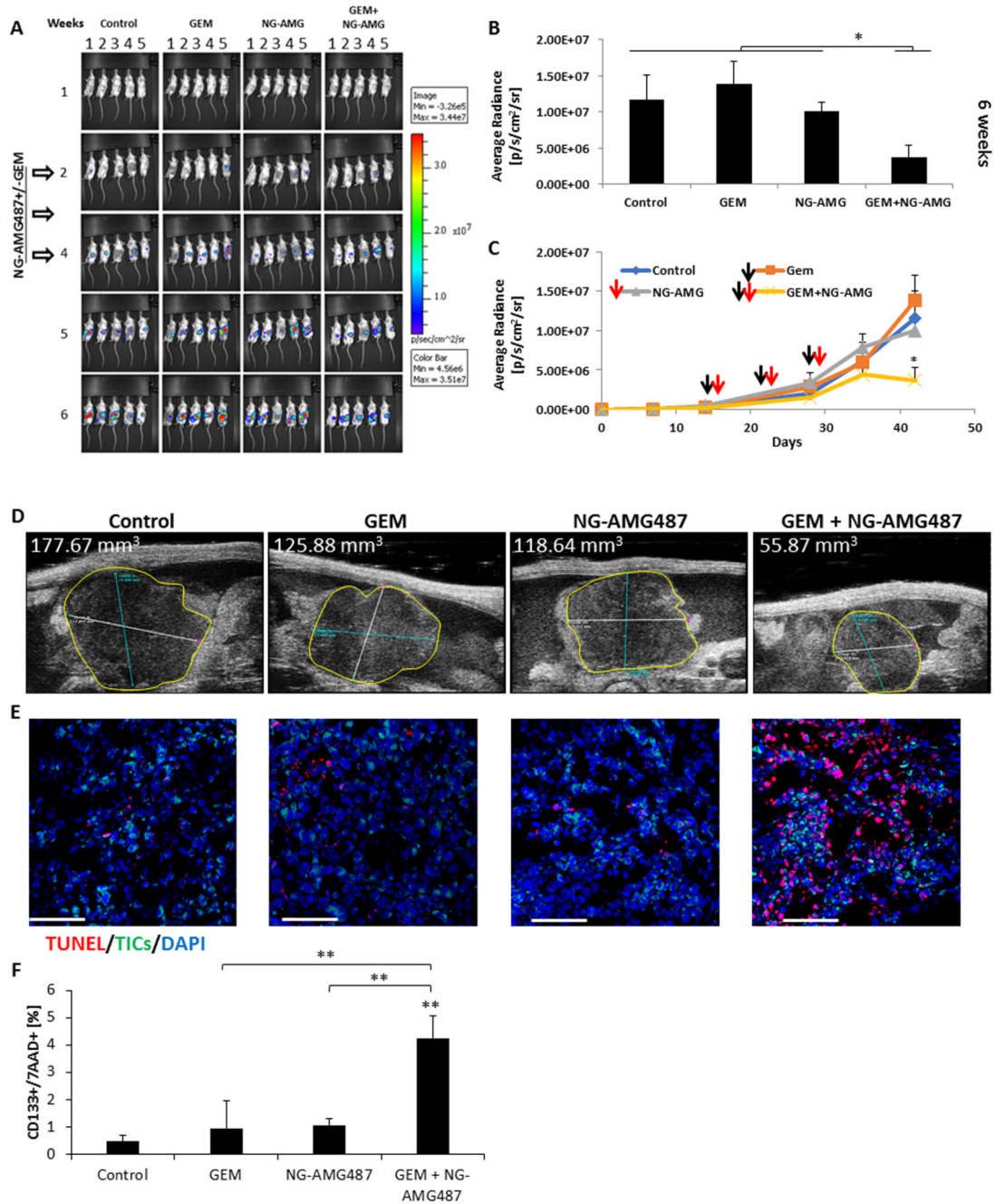


Figure 6. AMG487-loaded nano-ghosts inhibit tumor growth by inducing apoptosis: (A-D) Eight-to-ten week old SCID mice were orthotopically implanted with PANC1 cells (5×10^5 cells/mouse). After two weeks, mice were injected with gemcitabine chemotherapy (GEM, 500mg/kg), AMG487-loaded NG (NG-AMG487) or a combination of the two. Gemcitabine was injected weekly one day before the injection of NGs over a 3 week period (white arrows). Note, mouse 3 and 4 in control group week 6 exchanged position. (A) Tumor growth was assessed using the IVIS imaging system. (B-C) Shown are plots of bioluminescence levels. Black arrows represent gemcitabine injections and red arrows

represent NG-AMG487 injections. Error bars represent SE. (D) Tumor size at 6 weeks was also analyzed by micro-ultrasound. (E) At end point, tumors were removed. Half of each tumor was sectioned and the other half was prepared as a single cell suspension. Tumor sections were immunostained using antibodies against CD133 to detect TICs (green). Apoptotic cells were detected by TUNEL staining (red). Nuclei were stained with DAPI (blue). Scale bar, 100 μm . (F) The percentage of apoptotic TICs in single cell suspensions was evaluated by flow cytometry. * $p < 0.05$, ** $p < 0.01$, *** $p < 0.001$, as assessed by one way ANOVA followed by Tukey post-hoc test (when comparing between more than two groups).